Protoplasma (2008) 233: 61–72
DOI 10.1007/s00709-008-0307-x

PROTOPLASMA
Printed in Austria

Stringent control of cytoplasmic Ca^{2+} in guard cells of intact plants compared to their counterparts in epidermal strips or guard cell protoplasts

V. Levchenko[1,*], **D. R. Guinot**[2], **M. Klein**[3], **M. R. G. Roelfsema**[1], **R. Hedrich**[1], **P. Dietrich**[2]

[1] Molecular Plant Physiology and Biophysics, Julius von Sachs Institute for Biosciences, Würzburg University, Würzburg
[2] Molecular Plant Physiology, Erlangen-Nürnberg University, Erlangen
[3] Molecular Plant Physiology, Institute of Plant Biology, Zürich University, Zürich

Received 25 October 2007; Accepted 28 January 2008; Published online 22 July 2008
© Springer-Verlag 2008

Summary. Cytoplasmic calcium elevations, transients, and oscillations are thought to encode information that triggers a variety of physiological responses in plant cells. Yet Ca^{2+} signals induced by a single stimulus vary, depending on the physiological state of the cell and experimental conditions. We compared Ca^{2+} homeostasis and stimulus-induced Ca^{2+} signals in guard cells of intact plants, epidermal strips, and isolated protoplasts. Single-cell ratiometric imaging with the Ca^{2+}-sensitive dye Fura 2 was applied in combination with electrophysiological recordings. Guard cell protoplasts were loaded with Fura 2 via a patch pipette, revealing a cytoplasmic free Ca^{2+} concentration of around 80 nM at −47 mV. Upon hyperpolarization of the plasma membrane to −107 mV, the Ca^{2+} concentration increased to levels exceeding 400 nM. Intact guard cells were able to maintain much lower cytoplasmic free Ca^{2+} concentrations at hyperpolarized potentials, the average concentration at −100 mV was 183 and 90 nM in epidermal strips and intact plants, respectively. Further hyperpolarization of the plasma membrane to −160 mV induced a sustained rise of the guard cell cytoplasmic Ca^{2+} concentration, which slowly returned to the prestimulus level in intact plants but not in epidermal strips. Our results show that cytoplasmic Ca^{2+} concentrations are stringently controlled in guard cells of intact plants but become increasingly more sensitive to changes in the plasma membrane potential in epidermal strips and isolated protoplasts.

Keywords: Calcium; Calcium imaging; Fura 2; Guard cell; Impalement; patch clamp.

Introduction

Stomatal movements are influenced by extracellular Ca^{2+} (De Silva et al. 1985), which has been linked to the role of cytoplasmic Ca^{2+} concentrations in various guard cell responses. Changes in the cytoplasmic Ca^{2+} concentration affect ion channel activities and lead to altered ion fluxes, finally causing the guard cell volume to change (Blatt 2000, McAinsh et al. 2000, Hetherington 2001, Schroeder et al. 2001, Fan et al. 2004, Hetherington and Brownlee 2004, Roelfsema and Hedrich 2005). Various stimuli can induce either single or repetitive transient $[Ca^{2+}]_{cyt}$ rises, the mechanisms of which are complex and largely unknown. Due to the role of Ca^{2+} as an important second messenger the question emerges as to how stimulus specificity is obtained. In this context, the period of Ca^{2+} changes has been suggested to encode a signature that has the ability to trigger a specific response (McAinsh and Hetherington 1998, McAinsh and Stàxen 1999, Sanders et al. 1999, Trewavas 1999, Plieth 2001). Experiments with *Arabidopsis thaliana* guard cells in epidermal fragments revealed a correlation between the period of Ca^{2+} oscillations and the degree of stomatal closure (Allen et al. 2000, 2001). This correlation suggests that a stimulus-induced Ca^{2+} signature in guard cells encodes information that regulates stomatal movements.

Much of our knowledge of stimulus-induced Ca^{2+} responses in guard cells has been gained via microinjection of Ca^{2+}-sensitive ratiometric fluorescence dyes, such as Fura 2 (e.g., McAinsh et al. 1990) and Indo-1 (e.g., Gilroy et al. 1991), into guard cells of epidermal peels from *Commelina communis*. In addition, Ca^{2+} oscillations were studied using guard cells in epidermal fragments from *A. thaliana* acid loaded with Fura 2 (Allen et al. 1999a) or expressing the cameleon FRET reporter (Allen et al. 1999b). The various Ca^{2+} reporters

Correspondence: P. Dietrich, Molecular Plant Physiology, Friedrich-Alexander-Universität Erlangen-Nürnberg, Staudtstrasse 5, 91058 Erlangen, Federal Republic of Germany.
E-mail: dietrich@biologie.uni-erlangen.de
*Present address: V. Levchenko, Department of Physiology and Biochemistry of Plants, Belarusian State University, Minsk, Belarus.

revealed that repetitive Ca^{2+} transients and stomatal closure can be induced by the phytohormone abscisic acid (ABA), elevation of the extracellular Ca^{2+} concentration, oxidative stress, and cold treatment (Gilroy et al. 1991, McAinsh et al. 1995, Stàxen et al. 1999, Allen et al. 2000, Webb et al. 2001). However, in other experiments with epidermal strips and protoplasts, some of these stimuli were also found to induce single transients or a sustained rise in cytoplasmic Ca^{2+} (McAinsh et al. 1996, Webb et al. 1996, Romano et al. 2000). Apparently, the type of Ca^{2+} response depends on the physiological state of the cells or the experimental conditions (Allan et al. 1994).

Unlike in epidermal strips, ABA did not trigger repetitive rises in the cytoplasmic Ca^{2+} concentration of guard cells in intact plants (Levchenko et al. 2005, Marten et al. 2007). In *Vicia faba*, ABA triggered activation of plasma membrane anion channels in the absence of Ca^{2+} signals (Levchenko et al. 2005), whereas only single Ca^{2+} transients were observed in *Nicotiana tabacum* (Marten et al. 2007). Due to the latter variations, we set out to compare the regulation of cytoplasmic Ca^{2+} levels in guard cells in intact plants with those in epidermal strips and derived protoplasts. Electrophysiological methods were combined with the Ca^{2+} imaging technique to simultaneously monitor changes in cytoplasmic Ca^{2+} concentration and plasma membrane ion channel activity. From an in-depth in vivo calibration derived from Fura 2 excitation spectra in protoplasts and analysis of concentration-dependent buffering effects of the dye, we were able to show that this technique and our experimental conditions are appropriate for quantitatively comparing Ca^{2+} signals in guard cells under natural conditions and when separated from the leaf or even after removal of the cell wall. This is the first direct comparison of calcium homeostasis in guard cells of different preparations, i.e., the intact plant, epidermal strip, and isolated protoplasts.

Changes in the cytoplasmic Ca^{2+} concentration could be induced by manipulating the membrane voltage in all three systems, indicating the activity of voltage-dependent Ca^{2+} channels. Starting from similar resting $[Ca^{2+}]_{cyt}$, guard cells in intact plants elevated $[Ca^{2+}]_{cyt}$ only transiently upon hyperpolarization, while it remained elevated in epidermal strips. In guard cell protoplasts, $[Ca^{2+}]_{cyt}$ was extremely sensitive to variations in the membrane potential. From our results, we conclude that, moving from the intact system to the isolated protoplasts, $[Ca^{2+}]_{cyt}$ becomes more dependent on the plasma membrane potential and guard cells gradually lose their ability to reset $[Ca^{2+}]_{cyt}$ after voltage stimulation.

Material and methods

Plant material

Broad bean plants (*Vicia faba* L. cv. Französische Weisskeimige; Gebag, Hannover, Federal Republic of Germany) were grown in a greenhouse or climate chamber with a day–night cycle of 12 h light at 22 °C and 12 h dark at 16 °C. Leaves from 2- to 6-week-old plants were used.

Combined patch-clamp recordings and Ca^{2+} imaging

Isolation of guard cell protoplasts and patch-clamp recordings were performed as described previously (Dietrich et al. 1998), using an Axopatch 200A amplifier (Axon Instruments, Foster City, Calif., U.S.A.) and Pulse software (HEKA, Lambrecht, Federal Republic of Germany). Data were low-pass filtered at 2 kHz, sampled, digitized (ITC-16, Instrutech Corp., Elmont, N.Y., U.S.A.), stored on hard disk, and analyzed using Pulsefit software (HEKA). Protoplasts were loaded with Fura 2 (pentapotassium 2-[6-[bis(2-oxido-2-oxoethyl)amino]-5-[2-[2-[bis(2-oxido-2-oxoethyl)amino]-5-methylphenoxy]ethoxy]-1-benzofuran-2-yl]-1,3-oxazole-5-carboxylate) in the whole-cell configuration of the patch-clamp technique (see Fig. 2 A, C) by equilibration with pipette solution containing 150 mM K-gluconate, 10 mM KCl, 1 mM MgATP, 0.02 mM EGTA, 10 mM HEPES-Tris, pH 7.4, and 0.2 mM Fura 2–K_5. The standard bath solution was composed of 35 mM K-gluconate, 5 mM Ca-gluconate, and 10 mM morpholineethanesulfonic acid (MES)–Tris, pH 5.6 (for deviations, see figure legends). Solutions were adjusted to 400 mosmol/kg, using D-sorbitol. Voltages were corrected off-line for liquid junction potentials.

Fura 2 excitation was performed using a polychromator (VisiChrome; Visitron Systems GmbH, Puchheim, Federal Republic of Germany) coupled to the epifluorescence port of an inverted microscope (Axiovert 135; Zeiss GmbH, Jena, Federal Republic of Germany). Fluorescence emission was passed to the camera port of the microscope via a dichroic mirror and a bandpass filter (HQ535/50 nm; Chroma Technology Corp., Rockingham, Vt., U.S.A.), and images captured by a cooled digital camera system (−30 °C, CoolSNAP-HQ; Roper Scientific, Tucson, Ariz., U.S.A.). Excitation wavelengths, shutter, and image acquisition parameters were controlled via Metafluor software (Universal Imaging Corp., Downingtown, Pa., U.S.A.). For parallel patch-clamp and Fura 2 recordings, excitation and image acquisition were triggered by the Pulse patch-clamp software (HEKA) via TTL connections.

Pictures were taken at a resolution of 696 by 520 pixels (12 bit, 10 MHz pixel rate). Using a 40× lens (Plan Neofluar; aperture, 0.75; Zeiss GmbH), each pixel represented 0.32 μm^2. For time-dependent analysis of Ca^{2+} concentration changes, fluorescence intensities were averaged across the entire cell area, and background-corrected using a reference area outside the protoplast, as autofluorescence could be neglected.

For in vivo calibration, Fura 2 excitation spectra were assessed in the whole-cell configuration of the patch-clamp technique (Fig. 1 A). Due to optical constraints of the experimental setup, the maximum excitation of the Ca^{2+}-free dye at 335 nm (Grynkiewicz et al. 1985, Takahashi et al. 1999) was shifted to 354 nm. Instead of using the F_{340nm}/F_{380nm} ratio, we therefore used the F_{354nm}/F_{378nm} ratio in protoplasts as a measure for the cytoplasmic Ca^{2+} concentration. The ratio of the Ca^{2+}-bound and unbound Fura 2 forms (log[bound/free]) was plotted as a function of the free Ca^{2+} concentration (Fig. 1 B) revealing a K_d of 220 nM Ca^{2+}. This value is very similar to the K_d of 228 nM, as determined in vitro, using a calibration kit ($[Mg^{2+}]_{free}$ = 1 mM) and a UV-visible light spectrofluorimeter (American Instrument Co., Silver Spring, Md., U.S.A.; data not shown). Fluorescence ratios (F_{354}/F_{378}) were converted into actual $Ca^{2+}{}_{free}$ concentrations ($[Ca^{2+}]_{free}$) according to the following equation (Grynkiewicz et al. 1985):

$$[Ca]_{free} = K_d \frac{(R - R_{min})F_{min}}{(R_{max} - R)F_{max}}, \quad (1)$$

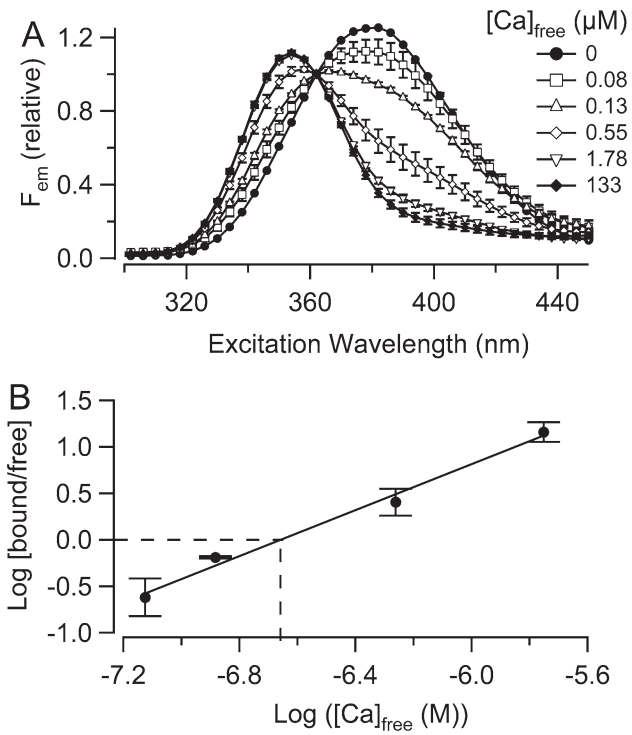

Fig. 1 A, B. In vivo calibration of Fura 2. **A** Fura 2 excitation spectra as determined in *V. faba* protoplasts in the presence of cytosolic free calcium concentrations buffered to values indicated (bars indicate SE, n = 3–5). At low $[Ca^{2+}]_{free}$, the Fura 2 excitation maximum is located at 378 nm, while it shifts to 354 nm in the Ca^{2+}-bound form. Data obtained from different cells were normalized to 360 nm. **B** Double logarithmic plot of the Ca^{2+}-bound versus Ca^{2+}-free Fura 2 concentration (log [bound/free]) as a function of the free calcium concentration. The crossing of the dotted line ([bound/free] = 1) with the abscissa indicates a K_d value of 220 nM $[Ca^{2+}]_{free}$

where K_d = 220 nM Ca^{2+}, $R = F_{354}/F_{378}$, $R_{min} = R$ at nominal zero Ca^{2+}, $R_{max} = R$ at saturating Ca^{2+}, and F_{min}/F_{max} is the fluorescence ratio of the unbound and bound forms of Fura 2, determined at 378 nm. Parameter values for F_{min} and R_{min} were determined with patch pipettes containing 10 mM EGTA, while R_{max} and F_{max} were measured with 0.02 mM EGTA and 1 mM Ca^{2+} in the pipette. The Fura 2-binding constant for Ca^{2+} (K_d) was determined in protoplasts with the standard pipette solution with EGTA increased to 10 mM. $[Ca]_{free}$ was varied between 0.014 and 133 μM using $CaCl_2$ according to the program Calcium.exe version 2.1 (W. Warchol, Poznan, Poland). Actual $[Ca]_{free}$ of the calibration patch solutions was determined with a Ca^{2+}-selective electrode (Carden and Felle 2003).

For image presentation for Fig. 5, individual wavelength pictures were averaged on a 3 × 3 scale, in order to improve the signal-to-noise ratio, and regions with signals <2 SD above background were discarded. After background correction, ratio images were generated and converted into colour-coded $[Ca^{2+}]_{free}$ values using the calibration parameters and Metamorph software (Universal Imaging Corp.).

Impalement studies

The youngest fully unfolded *V. faba* leaves were used for direct impalement with microelectrodes or for preparation of epidermal strips. Epidermal strips were peeled from the abaxial side of the leaf and glued with the cuticle side down to microscope slides using medical adhesive (Medical adhesive B liquid; Aromando Medizintechnik, Düsseldorf, Federal Republic of Germany). The microscope slide later became the bottom of the experimental chamber and the objective was moved from above into the solution of the chamber. In this configuration, the excitation and emission light did not pass the cuticle. For intact plants, the same microscope was used, but now light first had to pass the cuticle to reach the cytoplasm of the guard cell. The slides with epidermal strips were transferred to a petri dish with bath solution A (5 mM MES–Bis-Tris propane, pH 6.0, 5 mM KCl, and 1 mM $CaCl_2$). The epidermal strips were kept in the dark until use and measurements were carried out in the same bath solution, which could be exchanged for solutions with an altered $CaCl_2$ concentration at a rate of 0.5 ml/min, while the bath volume was kept at 0.4 ml. Recordings on guard cells in intact plants were carried out with leaves that were attached with their adaxial side to a Plexiglas holder, using double-sided adhesive tape. The holder was located in the focal plane of an upright microscope (Axioskop 2FS; Zeiss GmbH) and guard cells at the abaxial side of the leaf were visualized with a water immersion objective (Achroplan 40×; numerical aperture, 0.80; Zeiss GmbH). A drop of bath solution B (5 mM K citrate, pH 5.0, 5 mM KCl, 0.1 mM $CaCl_2$, and 0.1 mM $MgCl_2$) was placed between the objective and the cuticle (volume, 0.3 ml) and could be exchanged at a rate of 0.5 ml/min. The reference electrode, containing a 300 mM KCl and 0.1% agarose salt bridge, was placed in the bath solution (Roelfsema et al. 2001).

Triple-barrelled electrodes were pulled from borosilicate glass capillaries (outer diameter, 1.0 mm; inner diameter, 0.56 mm; Hilgenberg, Malsfeld, Federal Republic of Germany) that were aligned, heated, twisted 360°, and pulled on a customized vertical electrode puller (L/M-3P-A; List Medical Electronic, Darmstadt, Federal Republic of Germany) (Levchenko et al. 2005). The final pull was carried out on a horizontal laser puller (P-2000; Sutter Instruments, Novato, Calif., U.S.A.). Two barrels of the electrode were filled with 300 mM CsCl to block outward-rectifying K^+ channels, while the tip of the third barrel was filled with 2 mM Fura 2 and the rest of it with 300 mM CsCl. All three barrels of the microelectrode were connected via Ag/AgCl halfcells to microelectrode headstages (HS-180; Bio-Logic, Claix, France) with an input impedance of $>10^{-11}$ Ω, connected to microelectrode amplifiers (VF-102, Bio-Logic). Two barrels were used to measure and manipulate the guard cell membrane potential with a differential amplifier (CA-100, Bio-Logic) connected to an ITC-16 interface and controlled by Pulse software (HEKA). Current data were filtered with an 8-pole Bessel filter at 300 Hz and sampled at 1 kHz.

Fura 2 was loaded iontophoretically from the third barrel of the microelectrode, while the guard cell was clamped to −100 mV (see Fig. 2 B, D). In this configuration, loading currents up to −500 pA were automatically compensated by a current from the current injection barrel, thus preventing a potentially harmful hyperpolarization. Fura 2 concentrations were estimated by comparison of Fura 2-equilibrated guard cell protoplasts in the whole-cell configuration. Fura 2-based measurements were carried out at cytoplasmic concentrations ranging from 100 to 10 μM. Low cytoplasmic Ca^{2+} concentrations were obtained with simultaneous loading of Fura 2 and BAPTA (1,2-bis(*o*-aminophenoxy)ethane-N,N,N′,N′-tetraacetic acid) from the third microelectrode barrel at concentrations of 2 and 50 mM, respectively. Dual-excitation recordings using 200 ms light flashes were carried out at intervals of 1 s (Visitron Systems). Due to the optical properties of the Achroplan 40× (numerical aperture, 0.80) objective (Zeiss), the maximal changes in the Fura 2 ratio were obtained with excitation at 345 and 390 nm. The emission signal was filtered with a 510 nm bandpass filter (D510/40 M; AHF-Analysentechnik, Tübingen, Federal Republic of Germany) and captured with a cooled charge-coupled-device camera (CoolSNAP HQ, Roper Scientific). Background fluorescent signals for both excitation wavelengths were taken from a reference region in the unloaded neighbouring guard cell. Ratiometric values for the cytoplasmic free Ca^{2+} concentration were calculated with the Metafluor software (Universal Imaging). For

calculation of actual free Ca^{2+} concentrations, Eq. (1) was used, adopting a K_d value of 220 nM. In guard cells of epidermal strips and intact plants, F_{min} and R_{min} values were recorded after simultaneous injection of Fura 2 and BAPTA or clamping the membrane potential to 0 mV, respectively. F_{max} and R_{max} were obtained after clamping cells to −500 mV, which induced a large saturating rise in the Fura 2 ratio. The K_d value of 220 nM was also adopted for impaled guard cells, and using Eq. (1), we determined cytoplasmic free Ca^{2+} concentration for all three guard cell preparations, directly after ending the Fura 2 loading procedure.

Isolation of vacuoles and transport studies

Vacuoles were isolated from primary leaves of 8-day-old *Hordeum vulgare* var. Bakara plants according to published procedures (Klein et al. 1996). Vacuolar transport of 20 μM Fluo-3 or Fura 2 (Fluka, Buchs, Switzerland) salts was studied by the silicone-oil centrifugation technique as published earlier (Rentsch and Martinoia 1991, Klein et al. 1996) with a minor modification: 10 mM HEPES-KOH, pH 7.2, was used instead of water on top of the AR200 silicone oil (Fluka). For each condition and time point, six replicas were prepared. For quantification of vacuolar Fluo-3 and Fura 2, 60 μl of vacuolar supernatant was transferred into black OptiPlate-96F microplates (PerkinElmer, Zaventem, Belgium). Fluorescence emission was measured with a microplate analyzer (Packard, Meriden, Conn, U.S.A.) equipped with 485/20 or 340/10 nm excitation filters for Fluo-3 and Fura 2, respectively, and a 530/25 nm emission filter. Uptake rates were calculated as relative fluorescence per microliter of vacuolar volume determined by liquid scintillation counting of ^3H_2O in vacuolar supernatants and were corrected for unspecific binding. The presence of fluorochromes in vacuoles was further verified by recording the fluorescence emission spectra between 490 and 650 nm (excitation, 488 nm) or 400 and 650 nm (excitation, 340 nm) for Fluo-3 and Fura 2, respectively, of vacuolar samples and authentic standards dissolved in 10 mM HEPES-KOH, pH 7.2, with a PerkinElmer 3000 fluorescence spectrometer with slit widths set to 2.5 nm. All experiments were repeated twice with independent vacuole preparations.

If not stated otherwise, chemicals were purchased from Sigma-Aldrich (Taufkirchen, Federal Republic of Germany), apart from Fura 2, Fluo-3, and the Ca^{2+} calibration kit, which we obtained from Molecular Probes (Eugene, Oreg., U.S.A.).

Results

Fura 2-based Ca^{2+} recordings in guard cells

For estimation of the cytosolic Ca^{2+} concentration we used ratiometric imaging of the Ca^{2+}-sensitive fluorescent dye Fura 2. In guard cell protoplasts, Fura 2-based Ca^{2+} recordings were carried out in combination with the patch-clamp technique (Fig. 2 A), while Fura 2 was loaded with triple-barrelled intracellular microelectrodes

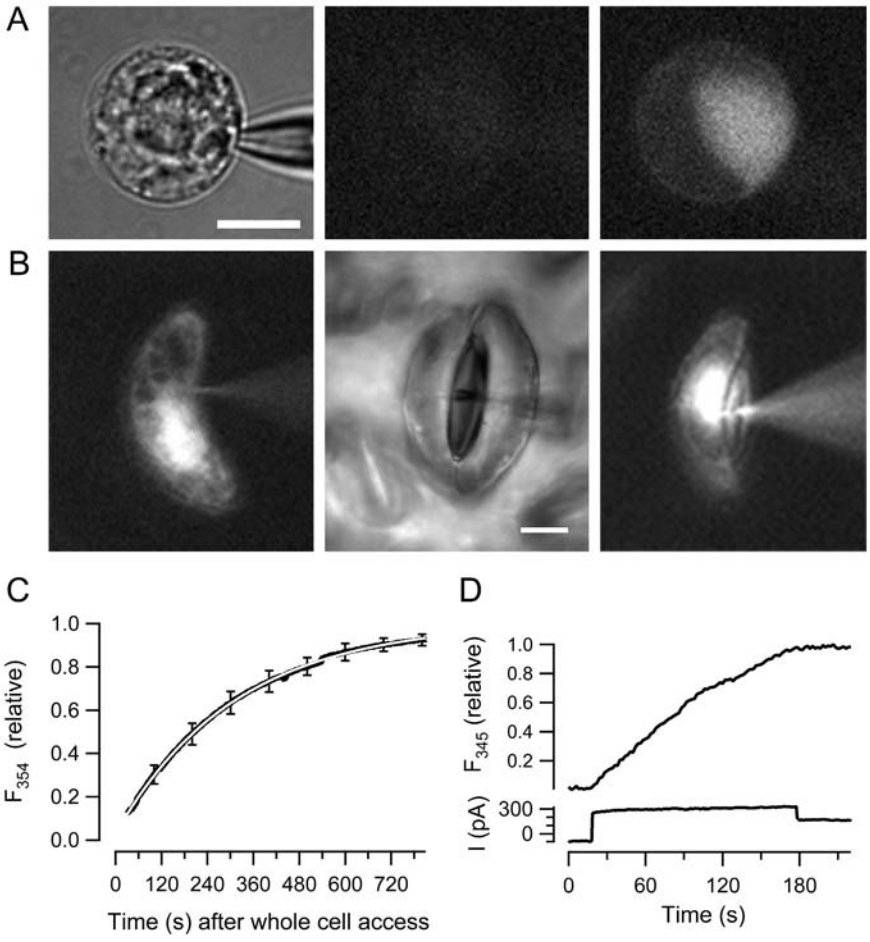

Fig. 2 A–D. Fura 2 loading into guard cells. **A** Transmitted-light (left) and fluorescence images of a guard cell protoplast before (middle) and after (right) loading of Fura 2 in the whole-cell configuration of the patch-clamp technique. Note the absence of interfering fluorescent signals emerging from chloroplasts (middle). The fluorescence of the patch pipette is not visible in this example, due to the focal plane. Bar: 10 μm. **B** Transmitted-light image of a stoma embedded in an intact plant (middle) and fluorescence images after Fura 2 loading via the impalement electrode into one guard cell of an epidermal strip (left) and an intact plant (right). **C** Kinetics of Fura 2 loading in guard cell protoplasts. Fluorescence at 354 nm (F_{354}) was normalized to the steady-state level at equilibrium (error bars represent SE, n = 18). The white line represents a single exponential fit function ($\tau = 5.1 \pm 1.4$ min). **D** Fluorescence increase (upper trace) during Fura 2 loading of a guard cell in an intact plant with a triple-barrelled microelectrode. The lower trace depicts the current applied via the second barrel, which compensates the Fura 2 injection current through the third barrel. F_{345} was normalized to its maximum value after loading

for guard cells in epidermal strips (Fig. 2 B, left) or intact plants (Fig. 2 B, right). Protoplasts were studied in the whole-cell configuration after equilibration with the Fura 2-containing patch solution (Fig. 2 C). Saturation of fluorescence intensities was reached 10 to 15 min after whole-cell access, with a time constant (τ) of 5.1 min (SE [standard error] = 1.4, n = 6), revealing that the equilibration process was slower than expected from diffusion (Pusch and Neher 1988). Guard cells in epidermal strips and intact plants were impaled through the cell wall facing the stomatal pore (Fig. 2 B). Fura 2 loading was started by application of an inward current (up to −500 pA) for several minutes through the injection barrel. During injection of Fura 2, the guard cells were constantly clamped to −100 mV and the injection current was compensated by a positive current via the second barrel (Fig. 2 D) (for loading dynamics, see supporting information in Levchenko et al. [2005]).

In protoplasts, Fura 2 fluorescence was concentrated in a restricted region, most likely related to the thin cytoplasm covering the unstained vacuole. In guard cells of epidermal strips and intact plants, the highest fluorescent signal was recorded from the central part (Fig. 2 B). No obvious difference in dye distribution was observed between guard cells in both preparations. The distribution of Fura 2 throughout the cells shows that the tip of the microelectrode was located in the cytoplasm. Both distant ends displayed low fluorescence intensity indicating vacuolar compartments (Fig. 2 B). In only one out of about 200 cells, a transient Fura 2 signal originated from a large compartment within the guard cell, probably due to impalement of the vacuole (data not shown).

In protoplasts clamped at −47 mV, the average Ca^{2+} concentration was 79 nM (SE = 11, n = 14). Guard cells in epidermal strips clamped to −100 mV maintained a cytoplasmic free Ca^{2+} concentration of 183 nM (SE = 27, n = 45), while that of cells in intact plants was 90 nM (SE = 10, n = 93). At the conditions applied, guard cells in all three preparations adjusted resting Ca^{2+} concentrations to between approximately 80 and 200 nM, well within the range determined by using different reporters, physiological conditions, or even cell types.

Time-dependent Fura 2 export from the cytoplasm

When Fura 2 loading was stopped in impalement experiments, or after patch excision from protoplasts, guard cells lost Fura 2 in time (Fig. 3 A). The rate of loss in intact guard cells of intact plants was higher than that in protoplasts, but similar to that in guard cells in epidermal strips. Loss of the Fura 2 signal did not depend on the period of excitation and thus probably was not due to photobleaching. Instead, guard cells seem to possess a detoxification mechanism that removes Fura 2 from the cytoplasm.

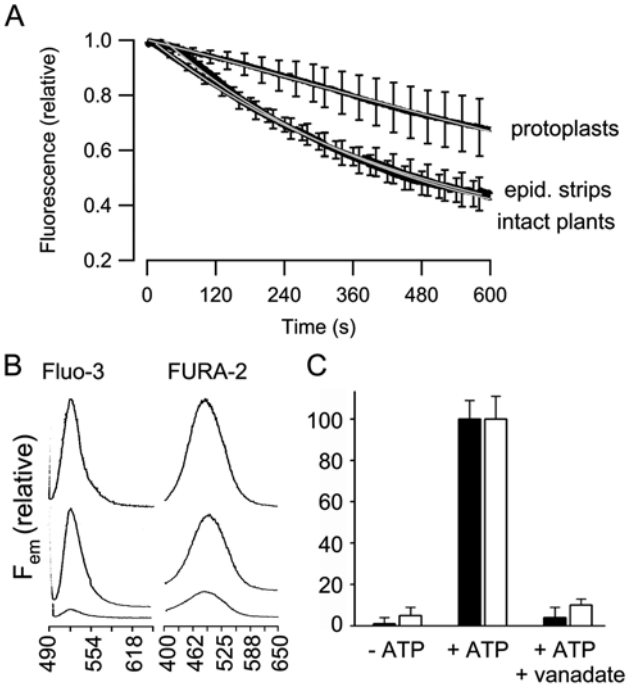

Fig. 3 A–C. Loss of Fura 2 from the cytoplasm and ATP-dependent dye transport into vacuoles. **A** Loss of Fura 2 fluorescence intensity in guard cells of intact plants, epidermal strips, and isolated protoplasts. Data represent mean of 5 (protoplasts) or 15 (epidermal peels or intact plant) measurements (with SE). The fluorescence decrease was continuously monitored in impaled guard cells after the Fura 2 loading procedure. In isolated protoplasts, the fluorescence decrease was recorded after patch excision. Grey lines represent fits of double exponential functions. **B** Barley mesophyll vacuoles were loaded for 18 min with 20 μM Fluo-3 (left) or Fura 2 (right) in the presence (middle traces) or absence (lower traces) of 3 mM MgATP. Fluorescence emission spectra were recorded with 488 nm (Fluo-3) and 340 nm excitation (Fura 2). Upper traces, spectra of authentic Fluo-3 and Fura 2 standards dissolved in 10 mM HEPES-KOH buffer, pH 7.2. **C** Transport rates for Fura 2 (open bars) and Fluo-3 (filled bars) in the presence (100%) and absence of 3 mM MgATP or with MgATP and vanadate

In plant vacuoles, carboxylated and sulfonated fluorescent dyes such as BCECF (Forestier et al. 2003) and Lucifer yellow CH (Klein et al. 1997) are transported into isolated vacuoles by ATP-dependent uptake mechanisms. We therefore tested if vacuoles could also take up the Ca^{2+} reporter dyes Fura 2 and Fluo-3. When isolated barley vacuoles were incubated with one of these Ca^{2+} reporter dyes, it accumulated in a MgATP-dependent manner (Fig. 3 B, C). Although the transport properties of vacuoles may differ between cell types and plant species, these results confirm that vacuoles transport a large vari-

ety of organic anions through ABC transporters (Forestier et al. 2003). It is, thus, very likely that guard cells lose Fura 2 due to the activity of these transporters.

Despite the uptake of Fura 2 into isolated vacuolar vesicles, Fura 2 signals were not detected in vacuoles of intact guard cells or protoplasts (Fig. 2 A, B), a finding in agreement with previous confocal images of guard cells, where the fluorescence was also excluded from vacuoles and chloroplasts (Gilroy 1997, Romano et al. 2000). The absence of visible fluorescence intensities from the vacuole may result from the dilution of the dye or the acidic luminal pH value affecting the fluorescence.

Extracellular Ca^{2+}-triggered rise in $[Ca^{2+}]_{cyt}$

Comparison of Ca^{2+} homeostasis required a stimulus that could be easily applied and reproducibly induce changes in $[Ca^{2+}]_{cyt}$. In previous studies, changes in the cytoplasmic Ca^{2+} concentration of guard cells in epidermal peels were induced through manipulation of the extracellular Ca^{2+} concentration (Gilroy et al. 1991, McAinsh et al. 1995, Webb et al. 2001). In *V. faba* guard cells in epidermal strips, elevation of the extracellular Ca^{2+} concentration from 1 to 10 mM caused a large rise in the cytoplasmic Ca^{2+} concentration, lasting as long as the stimulus was applied (Fig. 4 A, B). Guard cells in intact plants were also exposed to a rise in the Ca^{2+} concentration from 1 to 10 mM in the solution flowing on the cuticle. However, changing the Ca^{2+} concentration on the leaf surface had no effect on the Fura 2 ratio (Fig. 4 C). The lack of a response to high Ca^{2+} may be due to the large barrier that cuticles build for movement of Ca^{2+} (Schönherr 2000) or a decreased sensitivity to these ions in guard cells of intact plants.

Voltage-induced changes in $[Ca^{2+}]_{cyt}$

Hyperpolarization-induced rises in cytoplasmic Ca^{2+} have been observed in guard cells of epidermal strips and intact plants and thus may allow comparison of Ca^{2+} homeostasis in different preparations. In guard cell protoplasts, $[Ca^{2+}]_{cyt}$ reversibly rose during a 0.5 min voltage pulse from −47 to −107 or −127 mV (Fig. 5 A, C). The increase in $[Ca^{2+}]_{cyt}$ upon hyperpolarization was blocked by

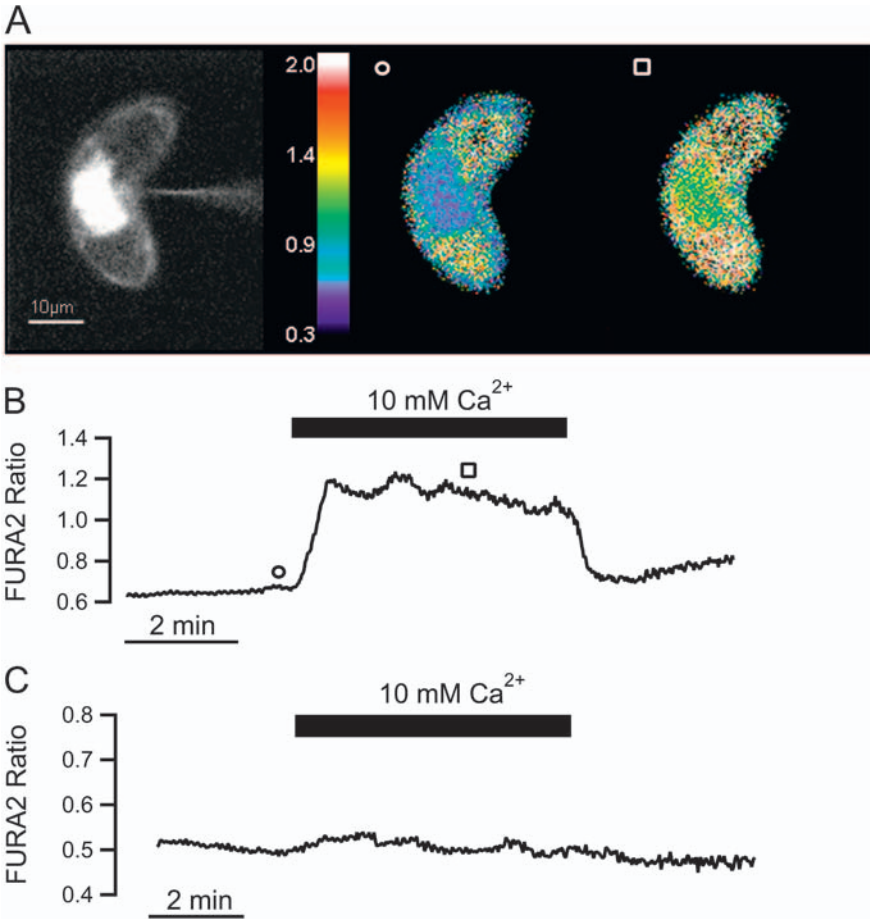

Fig. 4 A–C. External Ca^{2+}-induced $[Ca^{2+}]_{cyt}$ changes. **A** Fluorescence image (F_{390}) of a Fura 2-loaded guard cell in an epidermal strip and Fura 2 ratio images before (circles) and during (squares) external perfusion with 10 mM $CaCl_2$ in standard buffer (symbols correspond to those in **B**). The area surrounding the guard cell is shown in black, the position of the cell was determined from the fluorescence image on the left. **B** and **C** Time course of Fura 2 ratios before, during, and after 10 mM $CaCl_2$ treatment (black bars) of guard cells in an epidermal strip (**B**) or in a leaf of an intact plant (**C**). Data represent the average value of the Fura 2 F_{345}/F_{390} ratio from the cytoplasmic-rich bright fluorescent region in the centre of the cell. Traces are representative of 4 (epidermal strips) and 6 (intact plant) measurements

the Ca^{2+} channel inhibitor lanthanum. A concentration of 0.5 mM La^{3+} in the bath solution reduced $[Ca^{2+}]_{cyt}$ to resting values, as determined directly after dye loading (not shown here, i.e., 10–15 min after whole-cell access). However, La^{3+} had little effect on the inward currents (Fig. 5 A). A subsequent addition of 2 mM of the K^+ channel blocker Cs^+ (Hedrich et al. 1995, Dietrich et al. 1998) blocked inward-rectifying K^+ channels (Fig. 5 A, B).

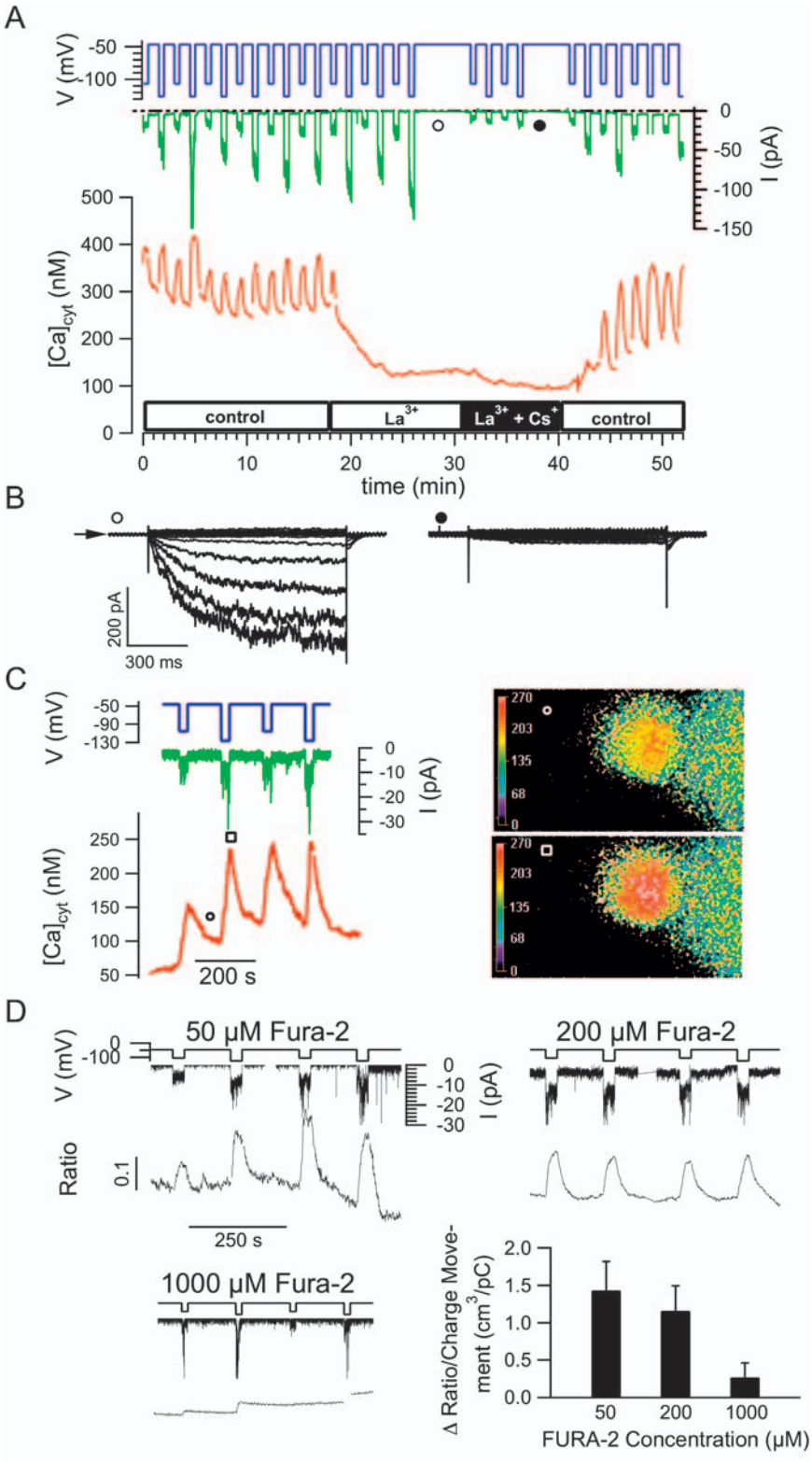

Fig. 5 A–D. Voltage-induced $[Ca^{2+}]_{cyt}$ changes and plasma membrane currents in guard cell protoplasts. **A** Guard cell protoplast stimulated with hyperpolarizing pulses. Voltage protocol (blue) and corresponding recordings of plasma membrane currents (green) and cytosolic Ca^{2+} concentrations (red) as determined from Fura 2 ratios according to Eq. (1). Currents and Ca^{2+} concentrations were recorded in standard bath solution (control), and after perfusion with additional 500 µM $LaCl_3$ in the absence (grey bar) and presence (black bar) of 2 mM $CsCl_2$. Note that inward currents are predominantly blocked by Cs^+, while Ca^{2+} elevations are prevented by La^{3+}. The block of currents and Ca^{2+} transients is reversed by perfusion with standard bath solution (control). **B** Whole-cell current response to voltages between +53 and −187 mV in 20 mV decrements, starting from a holding potential of −47 mV. Activation of inward-rectifying K^+ channels is induced by hyperpolarization in standard bath solution (open circle, symbols correspond to those in **A**). In the presence of 2 mM Cs^+ and 500 µM La^{3+}, K^+ channels are blocked (closed circle). Arrow indicates the zero current line. **C** Guard cell protoplast stimulated with hyperpolarizing pulses in the presence of Cs^+. Left, voltage protocol (blue) and corresponding recordings of plasma membrane currents (green) and cytosolic Ca^{2+} concentrations (red) in standard bath solution supplemented with 2 mM $CsCl_2$ to block inward-rectifying K^+ channels. Note that hyperpolarization-activated, Cs^+-insensitive currents become apparent. Right, pseudo-coloured images of $[Ca^{2+}]_{cyt}$ in guard cell protoplasts at −47 (upper image) and −127 mV (lower image). Symbols correspond to those in the Fura 2 ratio trace on the left. **D** Influence of increasing Fura 2 concentration on rises in cytoplasmic free Ca^{2+}. Starting from a holding potential of −47 mV, the plasma membrane of guard cell protoplasts was hyperpolarized to −107 and −127 mV (upper traces). The hyperpolarization induced an increase in plasma membrane currents (middle traces), and Fura 2 ratios (lower traces) were monitored. The standard pipette solution was supplemented with 50, 200, or 1000 µM Fura 2. Graph, the maximum ratio change induced by hyperpolarization from 3 voltage steps was averaged and related to the charge movement normalized to the protoplast volume. The latter was calculated from the slow membrane capacitance, with a specific value of 1 µF/cm^2. Data points represent the mean values (with SE, n = 5 [50 µM], n = 10 [200 µM], n = 3 [1000 µM])

This shows that inward K^+ channels, representing the major plasma membrane conductance at hyperpolarized voltages, are insensitive to the nonspecific cation channel blocker lanthanum at 0.5 mM, and do not contribute to hyperpolarization-induced Ca^{2+} entry. In response to increasingly negative voltage steps, Ca^{2+} permeates the membrane via a hyperpolarization-activated and La^{3+}-sensitive channel, and possibly through minor background conductances (Fig. 5 C). The effect of the Fura 2 concentration on hyperpolarization-induced Ca^{2+} changes was analyzed with different dye concentrations in the pipette (Fig. 5 D). A similar hyperpolarization-induced Ca^{2+} response was observed with 50 and 200 μM Fura 2, indicating a high Ca^{2+}-binding capacity of the guard cells (Zhou and Neher 1993). At 1 mM, Fura 2 significantly reduced the amplitude and decelerated the decay of the $[Ca^{2+}]_{cyt}$ signal. A comparison of the changes in the Fura 2 ratio signal and the charge that moved across the plasma membrane suggests that dye concentrations largely exceeding 200 μM should not be used.

In contrast to protoplasts, guard cells in epidermal strips or intact plants could be clamped to −100 mV in the absence of large rises in the cytoplasmic Ca^{2+} concentration. A further hyperpolarization of the plasma membrane to −160 mV initially caused an increase in the cytoplasmic Ca^{2+} concentration of guard cells in epidermal strips (Fig. 6 B, D), as well as in intact plants (Fig. 6 A, C, E). The Ca^{2+} concentration of guard cells

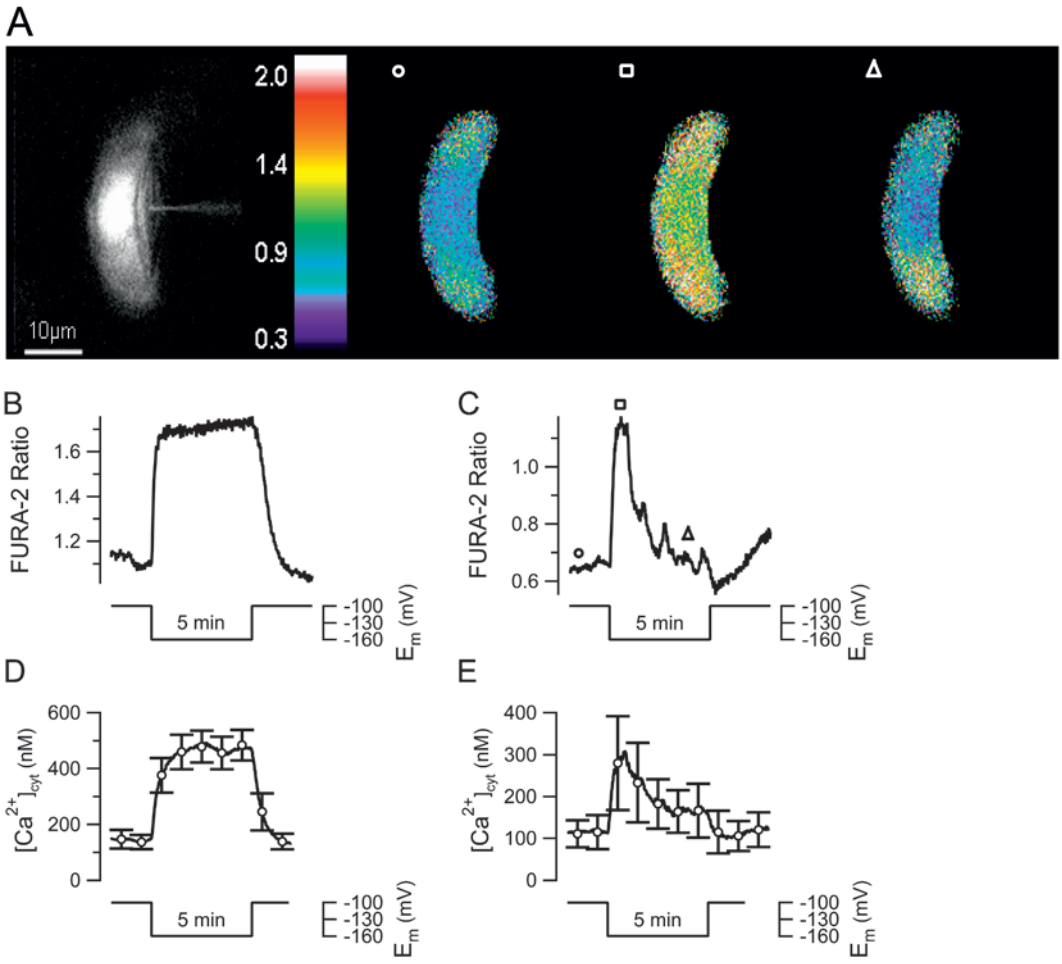

Fig. 6 A–E. Hyperpolarization-induced $[Ca^{2+}]_{cyt}$ changes. **A** Fluorescence image (F_{390}) and pseudo-coloured Fura 2 ratio images of a guard cell in an intact plant before and during a hyperpolarizing step to −160 mV. Symbols correspond to those in **C**. The area surrounding the guard cell is shown in black, the position of the cell was determined from the fluorescence image on the left. **B** and **C** Fura 2 ratios (upper traces) before, during, and after a 5 min voltage step from −100 to −160 mV in guard cells of an epidermal peel (**B**) and an intact plant (**C**). Data represent the average value of the Fura 2 F_{345}/F_{390} ratio from the cytoplasmic-rich bright fluorescent region in the centre of the cell. The lower traces indicate the membrane voltage during the experiment. **D** and **E** Mean $[Ca^{2+}]_{cyt}$ values from experiments shown in **B** and **C**, as calculated according to Eq. (1). Data points represent mean values (with SE) for guard cells in epidermal peels (n = 5) (**D**) and intact plants (n = 5) (**E**)

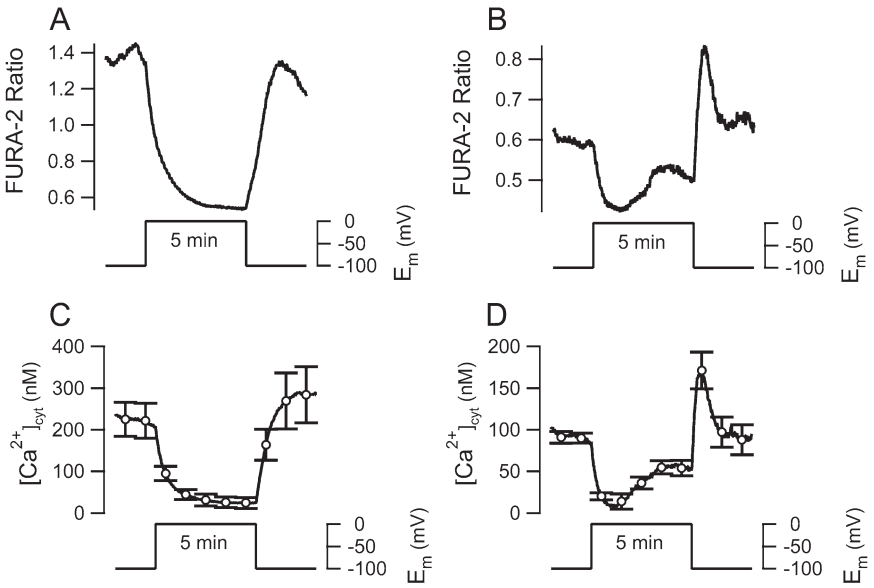

Fig. 7 A–D. Depolarization-induced $[Ca^{2+}]_{cyt}$ changes. **A** and **B** Fura 2 ratios (upper traces) before, during, and after a 5 min voltage step from −100 to 0 mV in guard cells of an epidermal strip (**A**) and an intact plant (**B**). The lower traces indicate the membrane voltage during the experiment. **C** and **D** Mean $[Ca^{2+}]_{cyt}$ values obtained from experiments shown in **A** and **B**, as calculated according to Eq. (1). Data points represent mean values (with SE) for guard cells in epidermal peels (n = 7) (**C**) and intact plants (n = 8) (**D**)

was not significantly different between epidermal strips and intact plants 30 s before and after hyperpolarization (t-test, $P > 0.5$). However, whereas the Ca^{2+} concentration remained elevated in epidermal strips (Fig. 6 B, D), it slowly returned to prestimulus values in intact plants (Fig. 6 C, E). As a result of this difference, $[Ca^{2+}]_{cyt}$ was significantly lower at the end of the hyperpolarizing pulse in guard cells of intact plants compared with those in epidermal strips (t-test, $P < 0.0056$). This suggests that guard cells in intact plants regulate the cytoplasmic Ca^{2+} concentration more tightly than those in epidermal strips.

Changes in $[Ca^{2+}]_{cyt}$ could be provoked not only with hyperpolarizing pulses but also with step pulses to more depolarized potentials (Fig. 7). Again, a difference was observed in the responses of guard cells in epidermal peels and intact plants. In epidermal peels, a change in the membrane potential from −100 to 0 mV led to a steady decrease in the cytoplasmic free Ca^{2+} concentration (Fig. 7 A, C), which was reversed again as the voltage was stepped back to −100 mV. A depolarization to 0 mV triggered an initial decrease in the cytoplasmic Ca^{2+} concentration of guard cells in intact plants as well, but in contrast to epidermal peels, this change was transient in nature (Fig. 7 B, D). Repolarization of the membrane potential to −100 mV caused an overshoot response; the cytoplasmic Ca^{2+} concentration transiently increased before returning to near the control level. Thus, compared to epidermal strips, guard cells in intact plants do not appear to tolerate long-term deviations from resting $[Ca^{2+}]_{cyt}$ induced by voltage changes. This points to a feedback control system, which is set to maintain $[Ca^{2+}]_{cyt}$ at a steady level in guard cells of intact leaves, but this system seems to operate less efficiently in guard cells of epidermal strips.

Discussion

Isolated guard cells do not resemble their counterparts in intact plants in all aspects (Willmer and Mansfield 1969, Roelfsema and Hedrich 2005), which prompted us to compare the Ca^{2+} homeostasis of these cells in three different physiological states. Here, Fura 2 was chosen as Ca^{2+} indicator, since this dye can be used in studies with guard cell protoplasts, as well as guard cells in epidermal strips or intact plants. In vivo calibration allowed us to quantitatively compare the Ca^{2+} homeostasis in guard cells of intact plants, in epidermal strips, and in guard cell protoplasts.

Hyperpolarization of the plasma membrane resulted in an initial increase in $[Ca^{2+}]_{cyt}$ in all three guard cell preparations. This is in line with the properties of Ca^{2+}-permeable cation channels that activate at potentials negative of −50 mV and are present in the plasma membrane of guard cell protoplasts (Hamilton et al. 2000, Pei et al. 2000). The weak voltage dependence of these channels explains how a depolarization from −100 to 0 mV initially causes a decrease in $[Ca^{2+}]_{cyt}$ in guard cells of epidermal strips and intact plants (Fig. 7), due to the closure of Ca^{2+} channels. Apparently, guard cells do not possess depolarization-activated Ca^{2+} channels (Thuleau et al. 1994).

Guard cell protoplasts displayed only a limited ability to control their cytoplasmic free Ca^{2+} concentration. Hyperpolarization of the plasma membrane to <-100 mV caused a rise in the cytoplasmic Ca^{2+} concentration, which could

only be reverted by repolarization of the membrane or by blocking the Ca^{2+} entry (Fig. 5). Compared to protoplasts, guard cells in epidermal strips impaled with microelectrodes were more efficient in keeping low $[Ca^{2+}]_{cyt}$, but still seemed to lack a slow Ca^{2+} feedback mechanism that is active in intact plants (Figs. 6 and 7). Hyperpolarization of the plasma membrane induced an initial rise in the cytoplasmic Ca^{2+} concentration in all guard cell preparations, which was followed by a slow return to a basic level only in intact plants, but not in epidermal strips. A similar difference was observed after a depolarization of the guard cell membrane. The slow recovery of $[Ca^{2+}]_{cyt}$ to the resting value points to a feedback mechanism that either inhibits the influx via plasma membrane cation channels or stimulates extrusion by Ca^{2+} transporters.

Ca^{2+} enters the cytoplasm of guard cells through Ca^{2+}-permeable cation channels that are stimulated at hyperpolarized potentials (Hamilton et al. 2000, Pei et al. 2000). These channels are effectively blocked by La^{3+}, but La^{3+} does not inhibit hyperpolarization-activated K^+ channels (Fig. 5). The open probability of the Ca^{2+}-permeable channels is suppressed by cytoplasmic Ca^{2+} (Hamilton et al. 2000), suggesting a feedback mechanism that limits the Ca^{2+} influx at high cytoplasmic Ca^{2+} concentrations. This channel-intrinsic property also operates in protoplasts and, therefore, is unlikely to account for the differences observed between protoplasts and guard cells in epidermal strips or intact plants. Additional feedback mechanisms may thus function in intact guard cells that are responsible for the slow attenuation observed after hyperpolarization (Fig. 6C, E) or depolarization (Fig. 7B, D).

Repetitive changes in $[Ca^{2+}]_{cyt}$ have been found with Fura 2-loaded guard cells of *C. communis* and cameleon-expressing guard cells of *A. thaliana* upon elevation of extracellular Ca^{2+} (McAinsh et al. 1995, Allen et al. 1999b), as well as hyperpolarization intervals induced by reducing the extracellular K^+-to-Ca^{2+} ratio (Allen et al. 2001). While we could mimic $[Ca^{2+}]_{cyt}$ oscillations by rapid voltage changes in all *V. faba* guard cell preparations, the increase in extracellular $[Ca^{2+}]$ caused a sustained rise in $[Ca^{2+}]_{cyt}$ in guard cells of epidermal strips and had no effect on guard cells of intact plants. Despite these differences, elevation of extracellular Ca^{2+} concentrations increased the basal level of $[Ca^{2+}]_{cyt}$ in guard cells of *C. communis* (McAinsh et al. 1995), *A. thaliana* (Allen et al. 1999b), and *V. faba* (this study). Thus, while the rise in basal $[Ca^{2+}]_{cyt}$ can be observed in all species, $[Ca^{2+}]_{cyt}$ oscillations vary between species and/or experimental conditions. The easiest explanation for this difference is to assume that $[Ca^{2+}]_{cyt}$ oscillations themselves are often due to rapid changes in membrane potential, gating voltage-dependent Ca^{2+} channels. In such a model, hyperpolarization induces the entry of Ca^{2+}, which in turn activates plasma membrane anion channels (Hedrich et al. 1990, Schroeder and Hagiwara 1990) that depolarize the cell and cause a decrease in $[Ca^{2+}]_{cyt}$ again. While in the former studies by McAinsh et al. (1995) and Allen et al. (1999b, 2001), $[Ca^{2+}]_{cyt}$ measurements were performed with free-running membrane potentials, we followed changes in $[Ca^{2+}]_{cyt}$ under voltage-clamp conditions. Changes in the free-running membrane potential are therefore very likely to shape repetitive $[Ca^{2+}]_{cyt}$ changes induced by physiological stimuli such as ABA (Stàxen et al. 1999) and CO_2 (Webb et al. 1996, Young et al. 2006).

The present study could unravel differences in Ca^{2+} feedback mechanisms, due to differences in the guard cell environment and preparation. Thus, the amplitude and kinetics of the calcium response, even under voltage-clamp conditions, is highly dynamic and not only varies between species (Levchenko et al. 2005, Marten et al. 2007) but also depends significantly on the experimental preparation (this study). It is likely that the feedback mechanisms regulating Ca^{2+}-permeable channels as well as intracellular Ca^{2+} transporters underlie these repetitive $[Ca^{2+}]_{cyt}$ changes. The role of vacuolar transporters in shaping the calcium response is supported by the altered Ca^{2+} homeostasis of guard cells in epidermal fragments of the *det3* mutant, which lacks a component of the V-type ATPase (Allen et al. 2000). Data on Ca^{2+} signals obtained with a certain experimental system may thus differ from those obtained for guard cells in other degrees of isolation from the intact plant.

Guard cells represent a highly specialized cell type but nevertheless remain totipotent in several plant species (Sahgal et al. 1994; Hall et al. 1996a, b). This shows that signals from neighbouring cells retain the guard cells in their differentiated state, but that dedifferentiation sets in after isolation. Upon isolation of a guard cell from the intact plant, communication will be lost and may induce slow alteration of the guard cell properties. Here, we have shown that guard cells in intact plants control $[Ca^{2+}]_{cyt}$ in a stringent manner, which is weakened in epidermal strips and lost to a further extent in protoplasts isolated from them. Changes in transcript levels have been shown to accompany the protoplast isolation procedure (Birnbaum et al. 2003), and differences in Ca^{2+} homeostasis of guard cells in intact plants and epidermal strips are also very likely reflected on the transcriptional level. Studying the pathways that lead to guard cell differentiation may thus identify proteins important for Ca^{2+} homeostasis in guard

cells and add to our understanding of calcium-based signalling events (Hetherington and Brownlee 2004) in these sensory cells.

Acknowledgements

We thank Ralf Steinmeyer (Zeiss, Göttingen) for discussions and initial help with the combined electrophysiology and fluorescence imaging measurements. We gratefully acknowledge Hubert Felle (University of Giessen) for determination of free Ca^{2+} concentrations in the calibration pipette solutions. V.L. and D.R.G. contributed equally to this work. It was supported by DFG grants (SPP1108) to R.H. and P.D. and by the SFB 567 grants to R.H. and M.R.G.R.

References

Allan AC, Fricker MD, Ward JL, Beale MH, Trewavas AJ (1994) Two transduction pathways mediate rapid effects of abscisic acid in *Commelina* guard cells. Plant Cell 6: 1319–1328

Allen GJ, Kuchitsu K, Chu SP, Murata Y, Schroeder JI (1999a) *Arabidopsis abi1-1* and *abi2-1* phosphatase mutations reduce abscisic acid-induced cytoplasmic calcium rises in guard cells. Plant Cell 11: 1785–1798

Allen GJ, Kwak JM, Chu SP, Llopis J, Tsien R-Y, Harper JF, Schroeder JI (1999b) Cameleon calcium indicator reports cytoplasmic calcium dynamics in *Arabidopsis* guard cells. Plant J 19: 735–747

Allen GJ, Chu SP, Schumacher K, Shimazaki CT, Vafeados D, Kemper A, Hawke SD, Tallman G, Tsien RY, Harper JF, Chory J, Schroeder JI (2000) Alteration of stimulus-specific guard cell calcium oscillations and stomatal closing in *Arabidopsis det3* mutant. Science 289: 2338–2342

Allen GJ, Chu SP, Harrington CL, Schumacher K, Hoffmann T, Tang YY, Grill E, Schroeder JI (2001) A defined range of guard cell calcium oscillation parameters encodes stomatal movements. Nature 411: 1053–1057

Birnbaum K, Shasha DE, Wang JY, Jung JW, Lambert GM, Galbraith DW, Benfey PN (2003) A gene expression map of the *Arabidopsis* root. Science 302: 1956–1960

Blatt MR (2000) Ca^{2+} signalling and control of guard-cell volume in stomatal movements. Curr Opin Plant Biol 3: 196–204

Carden DE, Felle HH (2003) The mode of action of cell wall-degrading enzymes and their interference with Nod factor signalling in *Medicago sativa* root hairs. Planta 216: 993–1002

De Silva DLR, Hetherington AM, Mansfield TA (1985) Synergism between calcium ions and abscisic acid in preventing stomatal opening. New Phytol 100: 473–482

Dietrich P, Dreyer I, Wiesner P, Hedrich R (1998) Cation sensitivity and kinetics of guard cell potassium channels differ among species. Planta 205: 277–287

Fan LM, Zhao Z, Assmann SM (2004) Guard cells: a dynamic signaling model. Curr Opin Plant Biol 7: 537–546

Forestier C, Frangne N, Eggmann T, Klein M (2003) Differential sensitivity of plant and yeast MRP (ABCC)-mediated organic anion transport processes towards sulfonylureas. FEBS Lett 554: 23–29

Gilroy S (1997) Fluorescence microscopy of living plant cells. Annu Rev Plant Physiol Plant Mol Biol 48: 165–190

Gilroy S, Fricker MD, Read ND, Trewavas AJ (1991) Role of calcium in signal transduction of *Commelina* guard cells. Plant Cell 3: 333–344

Grynkiewicz G, Poenie M, Tsien RY (1985) A new generation of Ca^{2+} indicators with greatly improved fluorescence properties. J Biol Chem 260: 3440–3450

Hall RD, Riksen-Bruinsma T, Weyens G, Lefebvre M, Dunwell JM, Krens FA (1996a) Stomatal guard cells are totipotent. Plant Physiol 112: 889–892

Hall RD, Riksen-Bruinsma T, Weyens GJ, Rosquin IJ, Denys PN, Evans IJ, Lathouwers JE, Lefebvre MP, Dunwell JM, van Tunen A, Krens FA (1996b) A high efficiency technique for the generation of transgenic sugar beets from stomatal guard cells. Nat Biotechnol 14: 1133–1138

Hamilton DW, Hills A, Köhler B, Blatt MR (2000) Ca^{2+} channels at the plasma membrane of stomatal guard cells are activated by hyperpolarization and abscisic acid. Proc Natl Acad Sci USA 97: 4967–4972

Hedrich R, Busch H, Raschke K (1990) Ca^{2+} and nucleotide dependent regulation of voltage dependent anion channels in the plasma membrane of guard cells. EMBO J 9: 3889–3892

Hedrich R, Moran O, Conti F, Busch H, Becker D, Gambale F, Dreyer I, Kuch A, Neuwinger K, Palme K (1995) Inward rectifier potassium channels in plants differ from their animal counterparts in response to voltage and channel modulators. Eur Biophys J 24: 107–115

Hetherington AM (2001) Guard cell signaling. Cell 107: 711–714

Hetherington AM, Brownlee C (2004) The generation of Ca^{2+} signals in plants. Annu Rev Plant Biol 55: 401–427

Klein M, Weissenböck G, Dufaud A, Gaillard C, Kreuz K, Martinoia E (1996) Different energization mechanisms drive the vacuolar uptake of a flavonoid glucoside and a herbicide glucoside. J Biol Chem 271: 29666–29671

Klein M, Martinoia E, Weissenbock G (1997) Transport of lucifer yellow CH into plant vacuoles – evidence for direct energization of a sulphonated substance and implications for the design of new molecular probes. FEBS Lett 420: 86–92

Levchenko V, Konrad K, Dietrich P, Roelfsema MRG, Hedrich R (2005) Cytosolic abscisic acid activates guard cell anion channels without preceding Ca^{2+} signals. Proc Natl Acad Sci USA 102: 4203–4208

Marten H, Konrad KR, Dietrich P, Roelfsema MRG, Hedrich R (2007) Ca^{2+}-dependent and -independent abscisic acid activation of plasma membrane anion channels in guard cells of *Nicotiana tabacum*. Plant Physiol 143: 28–37

McAinsh MR, Hetherington AM (1998) Encoding specificity in Ca^{2+} signalling systems. Trends Plant Sci 3: 32–36

McAinsh MR, Stàxen I (1999) Measurement of cytosolic-free Ca^{2+} in plant tissue. Methods Mol Biol 114: 307–321

McAinsh MR, Brownlee C, Hetherington AM (1990) Abscisic acid-induced elevation of guard cell cytosolic calcium precedes stomatal closure. Nature 343: 186–188

McAinsh MR, Webb AAR, Taylor JE, Hetherington AM (1995) Stimulus-induced oscillations in guard cell cytosolic free calcium. Plant Cell 7: 1207–1219

McAinsh MR, Clayton H, Mansfield TA, Hetherington AM (1996) Changes in stomatal behavior and guard cell cytosolic free calcium in response to oxidative stress. Plant Physiol 111: 1031–1042

McAinsh MR, Gray JE, Hetherington AM, Leckie CP, Ng C (2000) Ca^{2+} signalling in stomatal guard cells. Biochem Soc Trans 28: 476–481

Pei ZM, Murata Y, Benning G, Thomine S, Klusener B, Allen GJ, Grill E, Schroeder JI (2000) Calcium channels activated by hydrogen peroxide mediate abscisic acid signalling in guard cells. Nature 406: 731–734

Plieth C (2001) Plant calcium signaling and monitoring: pros and cons and recent experimental approaches. Protoplasma 218: 1–23

Pusch M, Neher E (1988) Rates of diffusional exchange between small cells and a measuring patch pipette. Pflugers Arch 411: 204–211

Rentsch D, Martinoia E (1991) Citrate transport into barley mesophyll vacuoles – comparison with malate-uptake activity. Planta 184: 532–537

Roelfsema MR, Hedrich R (2005) In the light of stomatal opening: new insights into 'the Watergate'. New Phytol 167: 665–691

Roelfsema MR, Steinmeyer R, Staal M, Hedrich R (2001) Single guard cell recordings in intact plants: light-induced hyperpolarization of the plasma membrane. Plant J 26: 1–13

Romano LA, Jacob T, Gilroy S, Assmann SM (2000) Increases in cytosolic Ca^{2+} are not required for abscisic acid-inhibition of inward K^+ currents in guard cells of *Vicia faba* L. Planta 211: 209–217

Sahgal P, Martinez GV, Roberts C, Tallman G (1994) Regeneration of plants from cultured guard cell protoplasts of *Nicotiana glauca* (Graham). Plant Sci 97: 199–208

Sanders D, Brownlee C, Harper JF (1999) Communicating with calcium. Plant Cell 11: 691–706

Schönherr J (2000) Calcium chloride penetrates plant cuticles via aqueous pores. Planta 212: 112–118

Schroeder JI, Hagiwara S (1990) Voltage-dependent activation of Ca^{2+}-regulated anion channels and K^+ uptake channels in *Vicia faba* guard cells. Am Soc Plant Physiol Symp Ser 4: 144–150

Schroeder JI, Allen GJ, Hugouvieux V, Kwak JM, Waner D (2001) Guard cell signal transduction. Annu Rev Plant Physiol Plant Mol Biol 52: 627–658

Stàxen I, Pical C, Montgomery LT, Gray JE, Hetherington AM, McAinsh MR (1999) Abscisic acid induces oscillations in guard-cell cytosolic free calcium that involve phosphoinositide-specific phospholipase C. Proc Natl Acad Sci USA 96: 1779–1784

Takahashi A, Camacho P, Lechleiter JD, Herman B (1999) Measurement of intracellular calcium. Physiol Rev 79: 1089–1125

Thuleau P, Moreau M, Schroeder JI, Ranjeva R (1994) Recruitment of plasma membrane voltage-dependent calcium-permeable channels in carrot cells. EMBO J 13: 5843–5847

Trewavas A (1999) Le calcium, c'est la vie: calcium makes waves. Plant Physiol 120: 1–6

Webb AAR, McAinsh MR, Mansfield TA, Hetherington AM (1996) Carbon dioxide induces increases in guard cell cytosolic free calcium. Plant J 9: 297–304

Webb AAR, Larman MG, Montgomery LT, Taylor JE, Hetherington AM (2001) The role of calcium in ABA-induced gene expression and stomatal movements. Plant J 26: 351–362

Willmer CM, Mansfield TA (1969) A critical examination of the use of detached epidermis in studies of stomatal physiology. New Phytol 68: 363–375

Young JJ, Mehta S, Israelsson M, Godoski J, Grill E, Schroeder JI (2006) CO_2 signaling in guard cells: calcium sensitivity response modulation, a Ca^{2+}-independent phase, and CO_2 insensitivity of the *gca2* mutant. Proc Natl Acad Sci USA 103: 7506–7511

Zhou Z, Neher E (1993) Mobile and immobile calcium buffers in bovine adrenal chromaffin cells. J Physiol 469: 245–273